Collective Synchronous Spiking in a Brain Network of Coupled Nonlinear Oscillators

Vitaly L. Galinsky and Lawrence R. Frank

Phys. Rev. Lett. **126**, 158102 — Published 16 April 2021

DOI: 10.1103/PhysRevLett.126.158102

Collective synchronous spiking in a brain network of coupled nonlinear oscillators

Vitaly L. Galinsky*
Center for Scientific Computation in Imaging, University of California at San Diego, La Jolla, CA 92037-0854, USA

Lawrence R. Frank†
Center for Scientific Computation in Imaging, University of California at San Diego, La Jolla, CA 92037-0854, USA and Center for Functional MRI, University of California at San Diego, La Jolla, CA 92037-0677, USA

(Dated: March 22, 2021)

A network of propagating nonlinear oscillatory modes (waves) in the human brain is shown to generate collectively synchronized spiking activity (hypersynchronous spiking) when both amplitude and phase coupling between modes is taken into account. The nonlinear behaviour of the modes participating in the network are the result of the non-resonant dynamics of weakly evanescent cortical waves that, as shown recently, adhere to an inverse frequency-wavenumber dispersion relation when propagating through an inhomogeneous anisotropic media characteristic of the brain cortex. This description provides a missing link between simplistic models of synchronization in networks of small amplitude phase coupled oscillators and in networks built with various empirically fitted models of pulse or amplitude coupled spiking neurons. Overall the phase–amplitude coupling mechanism presented in the Letter shows significantly more efficient synchronization compared to current standard approaches and demonstrates an emergence of collective synchronized spiking from subthreshold oscillations that neither phase nor amplitude coupling alone are capable of explaining.

Brain electromagnetic activity shows an abundance of oscillatory patterns across a wide range of spatial and temporal scales making the question of their interaction and synchronization an important issue that has been widely discussed in the literature [1]. All the typical approaches to the question of synchronization of multiple interconnected (neural)-networks can be divided into two big groups. The first approach works with network comprised of multiple harmonic oscillators in small (and constant) amplitude limit [2–8]. The second approach studies networks of multiple empirical nonlinear elements, e.g. various variants and simplifications of heavily over-fitted Hodgkin-Huxley neurons [9], including a multitude of ad hoc "integrate and fire" (IF) neuron models [1, 10–15]. Both approaches have there own advantages and drawbacks, but the main problem is that although they are often considered as complimentary, they are not just incompatible, they are based on contradictory assumptions. The first approach assumes that a phase of oscillations is the cornerstone of the synchronization process and all the importance of the amplitudes is second to none, hence the oscillating amplitudes can be safely assumed to be constant. The second approach on the contrary deems phase information to be nothing more then a sub-threshold noise that can be safely thrown away completely and just accumulates amplitudes of the arriving spikes or pulses when processing an input from multiple IF network members hoping that the discarded individual sub–spike phase information will magically be resurrected in a new form as population averaged synchronous phase.

Recently it was experimentally discovered that long–range (at the distance of 60mm apart or even more) correlations exist in human cortex in the 100-400Hz frequency range [16]. This frequency range corresponds to 2.5-10ms signal periods, i.e. it is at or even below duration of a single neuronal spike and, hence, it requires coherent spiking at the single neuron level and not just some average population synchrony. Neither of the two methods of phase coupled harmonic oscillators or pulse coupled IF neurons are capable of explaining this level of spiking synchrony as it is acknowledged in the literature that "there is no known mechanism through which the spikes of multiple neurons could be synchronized so precisely" [17].

The recently developed theory of weakly evanescent cortical waves (WETCOW) [18] provides a mechanism appropriate for explanation of long–range high frequency correlations and multiple wave modes and spikes synchronization up to and below single spike duration (hypersynchronous spiking) that follows directly from linear and nonlinear properties of wave modes. The linear wave dispersion relation predicts an inverse frequency–wavenumber dependence, hence the correlations at the highest frequencies should manifest themselves at the longest spatial scales in agreement with properties reported in [16]. The model of nonlinear interactions of those wave modes provides a mechanism of generation of spiking activity from their collective input, hence it is appropriate for explaining the physical origin of hypersynchronous spiking.

In this Letter we show that nonlinear model of brain wave modes developed in [18] can be reformulated using a simple but general Hamiltonian form that includes all possible nonlinear interaction at the lowest order of nonlinearity. Dynamical equations defined by this wave Hamiltonian reproduce oscillatory activity from linear (harmonic) wave regime to nonlinear spiking modes. Extending the Hamiltonian to include a pairwise coupling appropriate for a network of multiple nonlinear wave modes results in amplitude and phase coupled nonlin-

ear equations that show more efficient synchronization comparing to just phase coupling alone. For sufficiently strong coupling the spiking activity that emerges at different part of network from the small amplitude (below spiking detection or sub-threshold level) oscillations is synchronized not just in some averaged (spiking population) sense but at a single spike level. This amplitude/phase coupling approach thus provides a missing bridge between phase only coupling models of harmonic oscillator networks and amplitude (pulse) coupling models of IF neurons.

A nonlinear Hamiltonian form for an anharmonic oscillatory mode with a complex amplitude a in the lowest order of nonlinearity can be assumed to have an expression

$$H^s(a,a^\dagger) = \Gamma a a^\dagger + a a^\dagger \left[\beta_a a + \beta_{a^\dagger} a^\dagger - 2\alpha \left(a a^\dagger\right)^{1/2}\right] \quad (1)$$

where a is a complex oscillation amplitude and $a^\dagger$ is its conjugate. The first term $\Gamma a a^\dagger$ denotes the harmonic (quadratic) part of the Hamiltonian with the complex valued frequency $\Gamma = i\omega + \gamma$ that includes both a pure oscillatory frequency ω and a possible weakly excitation or damping rate γ. Because of the presence of this $\gamma \neq 0$, the conjugate † does not denote just the complex conjugate but more generally it also describes the growth or decay of the amplitude as a result of the presence of excitation or damping, e.g., for the growing oscillatory amplitude $a \sim e^{\gamma t + i\omega t}$ the conjugate will describe the correspondent decaying part as $a^\dagger \sim e^{-\gamma t - i\omega t}$.

The second anharmonic term (that is supposed to be cubic in the lowest order of nonlinearity) can be considered to include a product of the harmonic term $aa^\dagger$ and linear (in $|a|$) term that can be expressed in the most general form as $\beta_a a + \beta_{a^\dagger} a^\dagger - 2\alpha \left(aa^\dagger\right)^{1/2}$ (where α, β_a and $\beta_{a^\dagger}$ are the complex valued strengths of nonlinearity, and in general we do not assume that the Hamiltonian is in self–adjoint form, hence in general $\beta_a^\dagger \neq \beta_{a^\dagger}$). The terms with either a^3 or ${a^\dagger}^3$ do not appear in the Hamiltonian because for propagating waves they do not satisfy the wavenumber resonance conditions [18, 19].

It is worth noting that (1) is very general and can be used for a description of various anharmonic oscillatory physical processes valid to the lowest order of amplitude nonlinearity. In this Letter we have used it as a reformulation of weakly evanescent brain wave modes whose linear and nonlinear physical properties were presented in [18]. In this case, the nonlinear terms can be identified with the nonresonant interactions of linear wave modes propagating in either the same (β_a) or the opposite ($\beta_{a^\dagger}$) directions, or with the interactions with phase averaged nonpropagating modes (α).

An equation for the nonlinear oscillatory amplitude a then can be expressed as a derivative of the Hamiltonian form

$$\frac{da}{dt} = \frac{\partial H^s}{\partial a^\dagger} \equiv \Gamma a + 2\beta_{a^\dagger} a a^\dagger + \beta_a a^2 - 3\alpha a (a a^\dagger)^{1/2} \quad (2)$$

Substituting $a = \tilde{a}e^{i\omega t}$, $a^\dagger = \tilde{a}^\dagger e^{-i\omega t}$, $\beta_a = \tilde{\beta_a} e^{-i\delta_a}$, $\beta_{a^\dagger} = 1/2\tilde{\beta}_{a^\dagger} e^{i\delta_{a^\dagger}}$ and $\alpha = 1/3\tilde{\alpha}$, dropping the tilde, this can be rewritten as

$$\frac{da}{dt} = \gamma a + \beta_{a^\dagger} a a^\dagger e^{-i(\omega t - \delta_{a^\dagger})} + \beta_a a^2 e^{i(\omega t - \delta_a)} - \alpha a (a a^\dagger)^{1/2} \quad (3)$$

(3) is similar (up to the choice of the constants) to Eq. (29) of [18] but has an additional oscillatory term that was not included in [18]. Substituting in (2) $a = \tilde{a}e^{\gamma t + i\omega t}$ and $a^\dagger = \tilde{a}^\dagger e^{-\gamma t - i\omega t}$ instead of just the oscillatory complex exponents makes it is clear that those two terms represent the damped $\beta_{a^\dagger}\tilde{a}\tilde{a}^\dagger e^{-\gamma t - i(\omega t - \delta_{a^\dagger})}$ and the growing $\beta_a \tilde{a}^2 e^{\gamma t + i(\omega t - \delta_a)}$ parts of the nonlinear input and the spiking solutions can be obtained even when the damped term is neglected. Nevertheless, to analyze the more general case we will keep both of those terms and will show later that it is the asymmetry between those terms that provides an explanation for the presence of the phase difference that plays an important role in collective synchronization and hypersynchronous spiking.

Splitting (3) into an amplitude/phase pair of equations using $a = Ae^{i\phi}$ and assuming β_a, $\beta_{a^\dagger}$ and α to be real gives equations

$$\frac{dA}{dt} = \gamma A + A^2 \left(\beta_{a^\dagger} \cos\Omega_{a^\dagger} + \beta_a \cos\Omega_a - \alpha\right) \quad (4)$$

$$\frac{d\phi}{dt} = A\left(-\beta_{a^\dagger} \sin\Omega_{a^\dagger} + \beta_a \sin\Omega_a\right) \quad (5)$$

where $\Omega_a \equiv \Omega - \delta_a$, $\Omega_{a^\dagger} \equiv \Omega - \delta_{a^\dagger}$ and $\Omega \equiv \phi + \omega t$. These are similar to Eqs. (31) and (32) of [18] and show the same solution behaviour, i.e. transition from linear to nonlinear oscillation to spiking to non-oscillatory regime with an increase of excitation γ as it is evident from Fig.1 [20].

It should be noted that the asymmetries (i.e. the differences between the rising and the falling edges of the spikes) evident in the spiking solutions obtained both in Fig. 1 and in [18] (where additional asymmetric waveforms were presented) correspond to a special case that does not occur if a self–adjoint symmetry of the Hamiltonian form (1) is assumed. In a self–adjoint form (i.e. for $\beta_{a^\dagger} = \beta_a^\dagger$) the Hamiltonian in (1) can be alternatively expressed as

$$H^s(a,a^\dagger) = \Gamma a a^\dagger + a a^\dagger \left[F_+^2 + F_-^2\right] \quad (6)$$

where F_+ and F_- are defined as

$$F_+ = \sqrt{\beta_+^\dagger a^\dagger} + \sqrt{\beta_+ a} \quad (7)$$

$$F_- = \sqrt{\beta_-^\dagger a^\dagger} - \sqrt{\beta_- a} \quad (8)$$

and correspond to a symmetric ($F_+^\dagger = F_+$) and antisymmetric ($F_-^\dagger = -F_-$) combinations of the complex oscillatory modes a and $a^\dagger$, with complex parameters β_- and

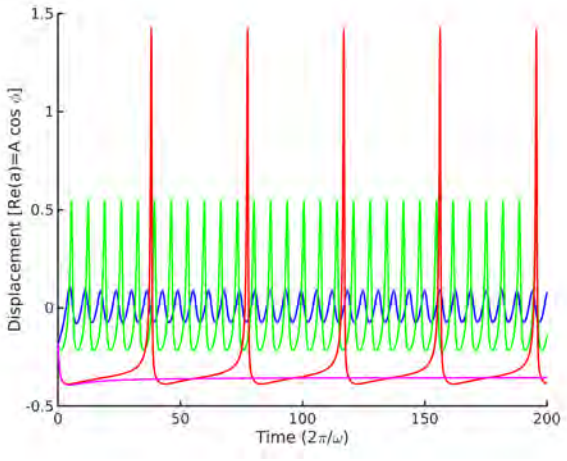

FIG. 1. Linear and nonlinear oscillations, spiking and non-oscillatory regime of solution of (4) and (5) at different levels of excitation ($\gamma = 0.25, 1, 1.98$ and 2:blue,green,red and magenta). Time is in the units of $2\pi/\omega$ and the amplitude a is in the arbitrary units. The rest of the parameters are the same for all plots: $\omega = 1$, $\beta_a = 2$, $\beta_{a^\dagger} = 1$, $\alpha = 3$, $\delta_{a^\dagger} = \pi/4$ and $\delta_a = -\pi/4$.

β_+ satisfying the relations

$$\beta_a = \beta_- + \beta_+, \quad \alpha = |\beta_-| - |\beta_+| \tag{9}$$

The parameters when the spiking solutions were obtained both in Fig. 1 and in [18] correspond to $\alpha > 0$, $\Rightarrow |\beta_-| > |\beta_+|$, $\Rightarrow |F_-| > |F_+|$ and the opposite case $|F_-| < |F_+|$ results in diverging solutions. The fixed difference in the power between $-$ and $+$ modes can be accompanied by various phase shifts, therefore we introduced those different δ_a and $\delta_{a^\dagger}$ phases in (3). As it was shown in [18] it is this difference in phases that is responsible for the asymmetries in the shape of spikes. Here we have augmented the theory presented in [18] to account for these phase differences as a consequence of symmetry considerations. Though the asymmetries in the spiking waveforms caused by this phase difference might appear subtle, this is important aspect of the theory as these asymmetries are observed experimentally [17]. but have not been explained by any existing theory. The effect on synchronization, however, is not subtle at all, as we demonstrate below.

These symmetry considerations create some (although very distant) analogy with symmetry differences between bosons and fermions. The antisymmetric form allows organization of the oscillations into highly ordered spike sequences. That is, it enforces in some sense the single oscillation quanta–single state "fermionic"–like selection rule by only allowing generation of a and $a^\dagger$ pairs. On the contrary, the symmetric form results in accumulation of oscillations in disordered divergent "bosonic" states. However the important point is that the observational fact of asymmetric spiking waveforms suggests the existence of distinct symmetric and anti-symmetric brain wave states. The origin of these is unknown.

As it was shown in [18] the spiking solution of Eqs. (31) and (32) of [18] (that are similar to the system (4) and (5) of this Letter) appears near the critical point where the oscillatory state undergoes bifurcation and transitions to a nonoscillatory regime as γ reaches the value above the critical point. Assuming as in [18] that the non–oscillatory regime requires that $dA/dt \to 0$ and $d\phi/dt \to -\omega$ (or $\phi \to -\omega t + \phi_0$, with ϕ_0 being some arbitrary phase) as $t \to \infty$, it is easy to see that the relative contribution of the excitation or damping in the amplitude exponents is proportional to γ/ω which is given by

$$\gamma/\omega = \frac{\alpha - \beta_{a^\dagger}\cos(\phi_0 - \delta_{a^\dagger}) - \beta_a \cos(\phi_0 - \delta_a)}{\beta_{a^\dagger}\sin(\phi_0 - \delta_{a^\dagger}) - \beta_a \sin(\phi_0 - \delta_a)}, \tag{10}$$

and for the parameters of Fig. 1 this defines a range $-2/5 < \gamma < 2$ with bifurcation at $\gamma_{crit} = 2$ in an excellent agreement with the transition from oscillatory to nonoscillatory regime obtained in numerical solutions of Fig. 1.

The Hamiltonian form for a network of multiple coupled "fermionic" state oscillators can then be written as

$$H(\boldsymbol{a}, \boldsymbol{a}^\dagger) = \sum_i \left[H^s(a_i, a_i^\dagger) + \sum_{j \neq i} \left(a_i r_{ij} a_j^\dagger + a_i^\dagger r_{ij}^* a_j \right) \right] \tag{11}$$

where $\boldsymbol{a} \equiv \{a_i\}$ and $r_{ij} = R_{ij} e^{i\Delta_{ij}}$ is the complex network adjacency matrix with R_{ij} providing the coupling power and Δ_{ij} taking into account any possible differences in phase between network nodes. And an equation for the complex amplitude a_i (again after a substitution of $a_i = \tilde{a_i} e^{i\omega_i t}$, $a_i^\dagger = \tilde{a_i}^\dagger e^{-i\omega_i t}$, $\beta_a = \tilde{\beta_a} e^{-i\delta_a}$, $\beta_{a^\dagger} = 1/2\tilde{\beta}_{a^\dagger} e^{i\delta_{a^\dagger}}$, $\alpha = 1/3\tilde{\alpha}$ and dropping the tilde)

$$\begin{aligned} \frac{da_i}{dt} &= \gamma_i a_i + \beta_{a^\dagger} a_i a_i^\dagger e^{-i(\omega_i t - \delta_{a^\dagger})} + \beta_a a_i^2 e^{i(\omega_i t - \delta_a)} \\ &\quad - \alpha a_i (a_i a_i^\dagger)^{1/2} + \sum_{j \neq i} r_{ij}^* a_j e^{i(\omega_j - \omega_i)t} \end{aligned} \tag{12}$$

now includes the coupling term. That gives for the amplitude A_i and the phase ϕ_i a set of coupled equations

$$\begin{aligned} \frac{dA_i}{dt} &= \gamma_i A_i + A_i^2 \left(\beta_{a^\dagger} \cos\Omega_{a^\dagger}^i + \beta_a \cos\Omega_a^i - \alpha \right) \\ &\quad + \sum_{j \neq i} R_{ij} A_j \cos(\Omega^j - \Omega^i - \Delta_{ij}), \end{aligned} \tag{13}$$

$$\begin{aligned} A_i \frac{d\phi_i}{dt} &= -A_i^2 \left(\beta_{a^\dagger} \sin\Omega_{a^\dagger}^i - \beta_a \sin\Omega_a^i \right) \\ &\quad + \sum_{j \neq i} R_{ij} A_j \sin(\Omega^j - \Omega^i - \Delta_{ij}). \end{aligned} \tag{14}$$

where $\Omega_a^i \equiv \Omega^i - \delta_a$, $\Omega_{a^\dagger}^i \equiv \Omega^i - \delta_{a^\dagger}$, $\Omega^i \equiv \phi_i + \omega_i t$, and the coupling terms are dependent upon $\Omega^j - \Omega^i =$

$(\phi_j - \phi_i) + (\omega_j - \omega_i)t$. In the small (and constant) amplitude limit (A_i = const) this set of equations turns into a set of phase coupled harmonic oscillators with a familiar $\sin(\phi_j - \phi_i \cdots)$ form of phase coupling. But in its general form (13) and (14) include also phase dependent coupling of amplitudes ($\cos(\phi_j - \phi_i \cdots)$) that dynamically defines if the input from j to i will either play excitatory ($|\phi_j - \phi_i + \cdots| < \pi/2$) or inhibitory ($|\phi_j - \phi_i + \cdots| > \pi/2$) roles (this is in addition to any phase shift introduced by the static network attributed phase delay factors Δ_{ij}).

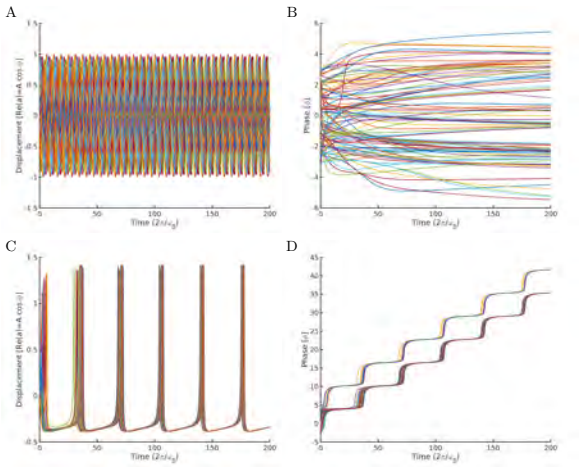

FIG. 2. Comparison of synchronization of phase-only constant amplitude harmonic oscillators (A,B) with amplitude-phase coupling of nonlinear (13) and (14) model (C,D). Network of 100 ring connected oscillators ($R_{ij} = 0.025$, $|i-j| \leq 2$ and $R_{ij} = 0$, $|i-j| > 2$) shows only transient weekly synchronized state (the order parameter $r = 0.32$) in the phase-only system (A,B) vs strongly synchronized spiking (the order parameter $r = 0.9999$ and still gradually increasing) in (C,D). Single frequency ($\omega \equiv \omega_0 = 1$) was used for both cases and $\beta_a = 2$, $\beta_{a^\dagger} = 1$, $\alpha = 3$, $\gamma = 1.875$, $\delta_{a^\dagger} = \pi/4$, $\delta_a = -\pi/4$ were the parameters for nonlinear (13) and (14) system.

The relatively simple set of equation (13) and (14) derived from the simple but nevertheless general Hamiltonian form (11) is capable to describe rich oscillatory and nonlinear dynamics as well as more efficient synchronization compared to phase-only coupled system of harmonic oscillators even for the relatively weak coupling. Fig. 2 shows comparison of synchronization in a weakly coupled network of phase-only constant amplitude harmonic oscillators vs amplitude and phase coupling of nonlinear system (13) and (14) [20]. The identical single frequency $\omega = \omega_0 = 1$ harmonic oscillators coupled in a ring with just 4 nearest neighbors ($R_{ij} = 0$, $|i-j| > 2$) is still showing a transient behaviour at $t = 200$ with the order parameter $r = 0.32$ (panels A and B) whereas the strongly synchronized spiking with mean frequency $\overline{\omega} \sim 0.175\omega_0$ is formed as early as about $t = 10$ for the nonlinear amplitude and phase coupling system (13) and (14) with the order parameter $r = 0.9999$ (panels C and D).

For a network with multiple individual frequencies

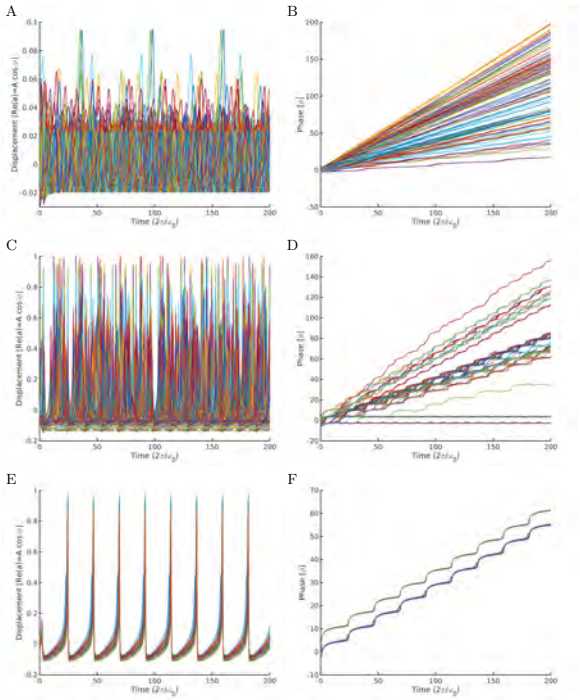

FIG. 3. Emergence of hypersynchronized spiking in a network of multiple frequency ($\omega_i < \omega_0 \equiv 1$, ω_i is uniformly distributed between 0.1 and 1, $\overline{\omega_i} = 0.54$, $\sigma_\omega = 0.25$) weakly forced ($\gamma_i = 0.25$) nonlinear oscillators. (A,B) shows low amplitude nonlinear oscillations of uncoupled set. (C,D) shows emergence of relatively weakly synchronized state with 3 distinct frequency groups at roughly 0, 0.3 and 0.6 plus some single elements at intermediate frequencies for a nearest neighbor random coupling ($R_{ij} = 0, |i-j| > 1$, $\overline{R_{ij}} = 1$, $\sigma_R = 0.415$). (E,F) shows emergence of strongly synchronized state with mean frequency at roughly ~ 0.5 and with the order parameter r=0.9882 for all to all random coupling $\overline{R_{ij}} = 0.01$, $\sigma_R = 0.0083$.

$\omega_i < \omega_0 \equiv 1$ uniformly distributed between $0.1\omega_0$ and ω_0 and with only a weak forcing at $\gamma_i = 0.25$, that is not sufficiently strong for generating spikes at individual uncoupled modes (as it can be seed from panels A and B of Fig. 3, where all the amplitudes of oscillations are below 0.1 and the phases are clearly showing the expected spread from 0.1 to 1, the order parameter r=0.0792), the coupling triggers collectively synchronized spiking at multiple frequencies (panels C and D) for a local nearest neighbor coupling or at a single mean frequency (panels E and F) for a global coupling (i.e. all–to–all or coupling of every node to all nodes in the network).

This level of synchronization effectiveness is maintained as a number of network nodes N increases and goes to infinity as can be seen in Fig. 4 (panel C). The network of Fig. 4 includes the large number of nodes $N = 10032$ split into 48 local groups located in different cortical regions (some of the nodes from several regions are shown in panel A) with 55mm the mean distance be-

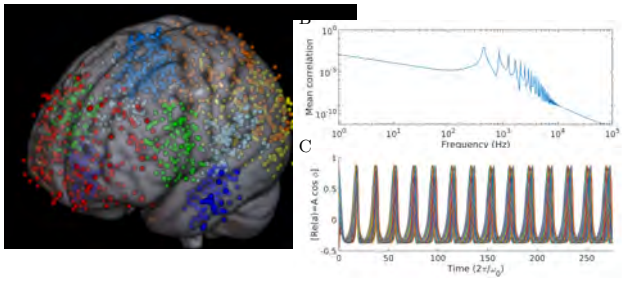

FIG. 4. (A) Network of $N = 10032$ nodes split in 48 local cortical regions with every node connected to 10-11 nodes from every other region. (B) The plot of pairwise correlations averaged across all nodes showing a peak at 300-500 Hz range in agreement with [16]. (C) Plot of synchronized oscillations.

tween regions (and 61mm the standard deviations). Each node is connected to 500 different nodes with 10-11 nodes from every region. The linear network frequencies are randomly distributed from 1Hz to 1KHz. A plot of pairwise node correlations averaged across all pairs (shown in panel B) clearly demonstrates the peak between 300 and 500 Hz in agreement with [16].

In conclusion, in this Letter we have presented a reformulation of the nonlinear model of weakly evanescent cortical wave (WETCOW) modes developed in [18] into a Hamiltonian form using a simple but general Hamiltonian representation that includes all possible nonlinear interactions at the lowest order of nonlinearity. Dynamical equations defined by this wave Hamiltonian reproduce oscillatory activity from the linear (harmonic) wave regime to nonlinear spiking modes. Extending the Hamiltonian to include a pairwise coupling appropriate for a network of multiple nonlinear wave modes results in amplitude and phase coupled nonlinear equations that show more efficient synchronization comparing to just phase coupling alone. For sufficiently strong coupling the spiking activity that emerges at different parts of network from the small amplitude (below spiking detection or sub-threshold level) oscillations is synchronized not just in some averaged (spiking population) sense but at a single spike resolution or below. This amplitude/phase coupling approach thus provides a missing link between phase only coupling models of harmonic oscillator networks and amplitude (pulse) coupling models of IF neurons, and has implications for understanding experimentally observed synchronous behaviour in the human brain.

LRF and VLG were supported by NSF grant ACI-1550405, UCOP MRPI grant MRP17454755 and NIH grant R01 AG054049.

* vit@ucsd.edu
† lfrank@ucsd.edu

[1] G. Buzsaki, *Rhythms of the Brain* (Oxford University Press, 2006); W. Gerstner, W. M. Kistler, R. Naud, and L. Paninski, *Neuronal Dynamics: From Single Neurons to Networks and Models of Cognition* (Cambridge University Press, New York, NY, USA, 2014).
[2] Y. Kuramoto, in *Mathematical Problems in Theoretical Physics*, Lecture Notes in Physics, Berlin Springer Verlag, Vol. 39, edited by H. Araki (1975) pp. 420–422.
[3] Y. Kuramoto and D. Battogtokh, Nonlinear Phenom. Complex Syst. **5**, 380 (2002).
[4] Y. Kuramoto, in *Nonlinear Dynamics and Chaos: Where do we go from here?*, edited by J. Hogan, A. Krauskopf, M. di Bernado, R. Wilson, H. Osinga, M. Homer, and A. Champneys (CRC Press, 2002) pp. 209–227.
[5] D. M. Abrams and S. H. Strogatz, Physical Review Letters **93**, 174102 (2004), nlin/0407045.
[6] J. A. Acebrón, L. L. Bonilla, C. J. Pérez Vicente, F. Ritort, and R. Spigler, Reviews of Modern Physics **77**, 137 (2005).
[7] D. Escaff and R. Delpiano, Chaos **30**, 083137 (2020).
[8] H. Wu, L. Kang, Z. Liu, and M. Dhamala, Sci Rep **8**, 15521 (2018).
[9] A. L. Hodgkin and A. F. Huxley, J. Physiol. (Lond.) **117**, 500 (1952).
[10] R. Fitzhugh, Biophys. J. **1**, 445 (1961).
[11] J. Nagumo, S. Arimoto, and S. Yoshizawa, Proceedings of the IRE **50**, 2061 (1962).
[12] C. Morris and H. Lecar, Biophys. J. **35**, 193 (1981).
[13] E. M. Izhikevich, IEEE Trans Neural Netw **14**, 1569 (2003).
[14] A. Kulkarni, J. Ranft, and V. Hakim, Front Comput Neurosci **14**, 569644 (2020).
[15] R. Kim and T. J. Sejnowski, Nat Neurosci **24**, 129 (2021).
[16] G. Arnulfo, S. H. Wang, V. Myrov, B. Toselli, J. Hirvonen, M. M. Fato, L. Nobili, F. Cardinale, A. Rubino, A. Zhigalov, S. Palva, and J. M. Palva, Nat Commun **11**, 5363 (2020).
[17] C. Gold, C. C. Girardin, K. A. Martin, and C. Koch, J Neurophysiol **102**, 3340 (2009).
[18] V. L. Galinsky and L. R. Frank, Physical Review Research **2**, 023061 (2020); J. of Cognitive Neurosci **32**, 2178 (2020).
[19] V. E. Zakharov, V. S. L'vov, and G. Falkovich, *Kolmogorov Spectra of Turbulence I: Wave Turbulence*, 1st ed., Springer Series in Nonlinear Dynamics (Springer-Verlag Berlin Heidelberg, 1992); S. Nazarenko, *Wave Turbulence*, 1st ed., Lecture Notes in Physics 825 (Springer-Verlag Berlin Heidelberg, 2011).
[20] See Supplemental Material at [URL will be inserted by publisher] for Wolfram Mathematica notebook with parameters and examples of numerical integration of systems (4), (5), (13) and (14) used for plots of Fig. 1 and Fig. 2.